Sulfuryl fluoride in the global atmosphere

JOURNAL OF GEOPHYSICAL RESEARCH, VOL. 114, D05306, doi:10.1029/2008JD011162, 2009

Sulfuryl fluoride in the global atmosphere

J. Mühle,[1] J. Huang,[2] R. F. Weiss,[1] R. G. Prinn,[2] B. R. Miller,[1,3] P. K. Salameh,[1] C. M. Harth,[1] P. J. Fraser,[4] L. W. Porter,[5,6] B. R. Greally,[7] S. O'Doherty,[7] and P. G. Simmonds[7]

Received 18 September 2008; revised 29 December 2008; accepted 2 January 2009; published 12 March 2009.

[1] The first calibrated high-frequency, high-precision, in situ atmospheric and archived air measurements of the fumigant sulfuryl fluoride (SO_2F_2) have been made as part of the Advanced Global Atmospheric Gas Experiment (AGAGE) program. The global tropospheric background concentration of SO_2F_2 has increased by 5 ± 1% per year from ~0.3 ppt (parts per trillion, dry air mol fraction) in 1978 to ~1.35 ppt in May 2007 in the Southern Hemisphere, and from ~1.08 ppt in 1999 to ~1.53 ppt in May 2007 in the Northern Hemisphere. The SO_2F_2 interhemispheric concentration ratio was 1.13 ± 0.02 from 1999 to 2007. Two-dimensional 12-box model inversions yield global total and global oceanic uptake atmospheric lifetimes of 36 ± 11 and 40 ± 13 years, respectively, with hydrolysis in the ocean being the dominant sink, in good agreement with 35 ± 14 years from a simple oceanic uptake calculation using transfer velocity and solubility. Modeled SO_2F_2 emissions rose from ~0.6 Gg/a in 1978 to ~1.9 Gg/a in 2007, but estimated industrial production exceeds these modeled emissions by an average of ~50%. This discrepancy cannot be explained with a hypothetical land sink in the model, suggesting that only ~2/3 of the manufactured SO_2F_2 is actually emitted into the atmosphere and that ~1/3 may be destroyed during fumigation. With mean SO_2F_2 tropospheric mixing ratios of ~1.4 ppt, its radiative forcing is small and it is probably an insignificant sulfur source to the stratosphere. However, with a high global warming potential similar to CFC-11, and likely increases in its future use, continued atmospheric monitoring of SO_2F_2 is warranted.

Citation: Mühle, J., et al. (2009), Sulfuryl fluoride in the global atmosphere, *J. Geophys. Res.*, 114, D05306, doi:10.1029/2008JD011162.

1. Introduction

[2] Sulfuryl fluoride (SO_2F_2) is used increasingly as a fumigant to replace methyl bromide, which, owing to its large ozone depletion potential, is being partially phased out (consumption for nonquarantine/preshipment uses) under the Montreal Protocol on Substances that Deplete the Ozone Layer and its subsequent amendments [*United Nations Environment Programme*, 2006]. During structural fumigation several thousand ppm (parts per million) of SO_2F_2 are applied over 24 h. Owing to its acute toxicity, SO_2F_2 levels within the fumigated structure must be reduced to less than 1 ppm prior to reentry by venting excess SO_2F_2 to the atmosphere (the exposure limit is 5–10 ppm). In addition, SO_2F_2 has been approved for postharvest fumigation of dried fruits, tree nuts, grains, and flours [*Environmental Protection Agency*, 2004, 2005]. SO_2F_2 has also been released in stack air (TRI Explorer, 2006, Environmental Protection Agency, http://www.epa.gov/triexplorer) (hereinafter Environmental Protection Agency online data, 2006), probably as a byproduct from certain manufacturing processes (M. Krieger, Dow AgroSciences, personal communication, 2008). Further emissions to the atmosphere may result from the use of SO_2F_2 in the semiconductor industry as a plasma cleaning gas [*Hobbs and Hart*, 2005] and in the magnesium industry as a blanketing gas to replace sulfur hexafluoride (SF_6), which has an exceptionally large global warming potential. Trace amounts of SO_2F_2 are also formed from SF_6 by electrical discharges in transformers [*Kóréh et al.*, 1997; *Pradayrol et al.*, 1997]. *Symonds et al.* [1988] concluded that SO_2F_2 emissions from volcanoes are probably extremely small. It is possible, however, that certain fluorite minerals may be a natural source of SO_2F_2 to the atmosphere [*Kranz*, 1966], similar to their roles as small sources of atmospheric carbon tetrafluoride (CF_4) and SF_6 [*Harnisch et al.*, 2000].

[1]Scripps Institution of Oceanography, University of California, San Diego, La Jolla, California, USA.
[2]Department of Earth, Atmospheric and Planetary Sciences, Massachusetts Institute of Technology, Cambridge, Massachusetts, USA.
[3]Now at Earth Systems, Research Laboratory, National Oceanic and Atmospheric Administration, Boulder, Colorado, USA.
[4]Centre for Australian Weather and Climate Research, CSIRO Marine and Atmospheric Research, Aspendale, Victoria, Australia.
[5]Bureau of Meteorology, Melbourne, Victoria, Australia.
[6]Deceased 7 December 2007.
[7]School of Chemistry, University of Bristol, Bristol, UK.

0148-0227/09/2008JD011162$09.00

[3] From a recent European Union report [*Swedish Chemicals Agency*, 2005] a global anthropogenic release of 1.8 Gg/a can be deduced for 1992 to 2000, on the basis of estimates of global SO_2F_2 production and release provided by Dow AgroSciences. This report also estimates that more than 88% of SO_2F_2 emitted to the atmosphere, more than 1.62 Gg per year, results from fumigant use and that the atmospheric lifetime of SO_2F_2 is at most 4.5 years. This lifetime estimate is an upper limit obtained from a global mass balance calculation, based on a steady state assumption for an SO_2F_2 mixing ratio of at most 0.5 ppt (the detection limit of earlier measurements which failed to detect SO_2F_2 in background air). It is assumed in this report that SO_2F_2 does not react with the OH radical, that wet and dry deposition are negligible, that uptake and degradation by vegetation and soils are possible but unquantified sinks, and that hydrolysis in surface waters and photodissociation in the stratosphere are likely significant sinks of SO_2F_2 [*Swedish Chemicals Agency*, 2005].

[4] According to the California Pesticide Use Reports (1989–2006, from California Environmental Protection Agency, http://www.cdpr.ca.gov/docs/pur/purmain.htm) (hereinafter California Environmental Protection Agency online reports, 1989–2006), the pesticide use of SO_2F_2 in California has increased from 0.44 to 1.30 Gg/a from 1989 to 2006, and was used mostly for structural pest control (S. Orme and S. Kegley, PAN Pesticide Database, 2006, http://www.pesticideinfo.org; see also California Environmental Protection Agency online reports, 1989–2006) and was therefore eventually emitted into the atmosphere [*Swedish Chemicals Agency*, 2005]. For 2000, this report [*Swedish Chemicals Agency*, 2005] states that 1.1 Gg of SO_2F_2 were used in California as pesticide, corresponding to 60% of the global anthropogenic estimate given above.

[5] SO_2F_2 is registered for fumigation use in the United States, Canada, the Caribbean, Japan, Australia (in 2008), Switzerland, and the European Union [e.g., *Derrick et al.*, 1990; *United Nations Environment Programme*, 2004], so that future emissions will most likely increase. SO_2F_2 is currently produced in the United States (Dow AgroSciences), China (Zhejiang Linhai Liming Chemical Co. and LongKou City Chemical Plant), Germany (Solvay), and Poland (Fluorochemika).

[6] The environmental fate of SO_2F_2 is poorly known. In the troposphere it is likely removed very slowly by reaction with OH or NO_3 radicals or O_3, as SO_2F_2 is highly oxidized and much more chemically inert than other oxidized sulfur gases such as SO_2Cl_2 [*Holleman and Wiberg*, 1985]. Motivated by our initial atmospheric measurements [*Mühle et al.*, 2006], kinetic studies of SO_2F_2 have been performed by *Dillon et al.* [2008] and, in a collaborative effort with us, by *Papadimitriou et al.* [2008]. These studies confirm that gas-phase reactions of SO_2F_2 with Cl, O_3, and $O(^1D)$ are unimportant, and that the reaction with OH is, at most, marginally important.

[7] The solubility of SO_2F_2 in water per atmosphere (atm) partial pressure is 0.529 cm^3 (STP)/mL at 0°C and 0.215 cm^3 (STP)/mL at 23.3°C [*Cady and Misra*, 1974], which equates to 2.41 g/L and 0.978 g/L, respectively. (Published solubility constants ~16 times lower likely resulted from the incorrect use of the vapor pressure of SO_2F_2 (15.6 atm) in the calculation, even though the experiment was performed at 1 atm (M. Krieger, Dow AgroSciences, personal communication, 2007).) *Holleman and Wiberg* [1985] report that SO_2F_2 does not decompose in the presence of water up to 150°C, while *Cady and Misra* [1974] state that SO_2F_2 hydrolyzes slowly in water and quickly in basic solutions. Therefore hydrolysis in acidic environments such as most precipitation [*Whelpdale and Miller*, 1989; *Collett et al.*, 1994; *Seinfeld and Pandis*, 1997] and many lakes and rivers is likely unimportant, while hydrolysis in the slightly basic surface ocean waters [*Orr et al.*, 2005] could affect the atmospheric lifetime of SO_2F_2 significantly [*Cady and Misra*, 1974].

[8] SO_2F_2 does not photolyze in the lower atmosphere, but in the upper atmosphere it will eventually be photolyzed by hard UV radiation or removed by ion and radical processes [*Pradayrol et al.*, 1996; *Dillon et al.*, 2008; *Papadimitriou et al.*, 2008] similar to those that remove trifluoromethyl sulfur pentafluoride (SF_5CF_3) [*Takahashi et al.*, 2002a] or SF_6 [*Ravishankara et al.*, 1993; *Morris et al.*, 1995].

[9] SO_2F_2 can be a source of stratospheric sulfur [*Crutzen*, 1976] and a "greenhouse gas" [*California Environmental Protection Agency*, 2005; *Pest Management Regulatory Agency*, 2006] owing to its infrared absorption in the "atmospheric window" [*Perkins and Wilson*, 1952; *Hunt and Wilson*, 1960; *Heise et al.*, 1997; *Dillon et al.*, 2008; *Papadimitriou et al.*, 2008].

[10] In this paper we present the first calibrated high-frequency, high-precision, in situ ambient and archive air measurements of SO_2F_2, reconstruct the global atmospheric history, discuss the sink processes, estimate the atmospheric lifetime, quantify the source flux, and discuss the importance of SO_2F_2 as a sulfur source to the stratosphere and as an infrared-absorbing "greenhouse gas."

2. Experimental Method

2.1. Instrumentation and Calibration

[11] Sulfuryl fluoride and ~35 other halogenated compounds are measured by the Advanced Global Atmospheric Gases Experiment (AGAGE) in 2-L air samples with the newly developed Medusa instrument, a cryogenic preconcentration system custom-fitted to a gas chromatograph (GC, Agilent 6890) with a quadrupole mass selective detector (MSD, Agilent 5973) [*Miller et al.*, 2008].

[12] For this work, data from seven Medusa GC/MSD instruments at seven sites were used. The La Jolla (33°N, 117°W, California) site at the Scripps Institution of Oceanography (SIO) serves as the main calibration site. Archived air tanks (see section 2.3) were measured at SIO and at the Commonwealth Scientific and Industrial Research Organisation (CSIRO, Aspendale, Australia). Routine ambient air measurements began at SIO in August 2004, and subsequently at the five remote AGAGE field stations: at Mace Head, Ireland (53°N, 10°W) in November 2004; at Trinidad Head, California (41°N, 124°W) in April 2005; at Cape Grim, Tasmania (41°S, 145°E) in May 2005; at Ragged Point, Barbados (13°N, 59°W) in July 2005; and at Cape Matatula, American Samoa (14°S, 171°W) in June 2006.

[13] Each ambient or archived air sample was alternated with reference gas measurements [*Prinn et al.*, 2000], resulting in up to 12 fully calibrated air measurements per

day. The reference gases at each site were calibrated relative to parent standards at SIO. Details of the calibration method and hierarchy are given by *Miller et al.* [2008].

[14] SO_2F_2 is reported on the SIO-2007 scale, which is based on gravimetric SO_2F_2/nitrous oxide (N_2O) mixtures prepared via a stepwise dilution technique with large dilution factors for each step in the range of 10^3 to 10^5 [*Prinn et al.*, 2000, 2001] to reduce systematic uncertainties. The SIO-2007 SO_2F_2 scale is based on four stable primary calibration standards in zero air with prepared values of 3.30–3.41 ppt, each containing ~20 torr water vapor. Each zero air/water vapor primary was measured on the Medusa GC/MSD to verify insignificant SO_2F_2 blank levels before being spiked with one of the SO_2F_2/N_2O mixtures. For further calibration details, see *Prinn et al.* [2000]. The pure SO_2F_2 (99.8%, Dow AgroSciences) and N_2O (99.99%, Matheson or 99.99997%, Scott Specialty Gases) used to prepare the primary standards were further purified by repeated cycles of freezing (at −196°C), vacuum removal of noncondensable gases, and thawing. Zero air (Ultra Zero Grade, Airgas) was further purified via an absorbent trap filled with glass beads, Molecular Sieve (MS) 13X, charcoal, MS 5Å, and Carboxen 1000 at ethanol/dry ice temperature. The earlier calibration used by *Mühle et al.* [2006] was based on an approximate 80 ppt volumetric mixture which the present gravimetric standards show to have given atmospheric SO_2F_2 value that were too low by a factor of 1.42.

[15] Typical daily precisions of reference gas measurements are 0.01–0.03 ppt. SO_2F_2 measurements were linear within 2–3% over 2 orders of magnitude [*Miller et al.*, 2008]. Replicate analysis of archived air samples over a time period of up to almost 4 years typically agree within 0.01–0.02 ppt showing that SO_2F_2 is stable in these tanks. Detection limits for 2-L ambient air samples are 0.02–0.04 ppt (3 times baseline noise). Typically the analytical system showed no blanks for SO_2F_2. Previously used analytical methods including gas chromatography with various detectors achieved detection limits in the 1- to 20-ppm range [*Kóréh et al.*, 1997; *Pradayrol et al.*, 1997], except for *Qu et al.* [2000], who reported a detection limit of 0.4 ppt by GC-ECD (electron capture detector).

2.2. Mass Spectrometric Identification

[16] SO_2F_2 was first detected with the MSD at SIO as a peak of highly variable size eluting from the chromatographic main column (CP-PoraBOND Q, 0.32 mm ID, 25 m, 5 μm, Varian Chrompack) shortly after CFC-13 ($CClF_3$), and with the same mass to charge ratio (m/z) 85 used to quantify CFC-13. Mass spectra obtained in the highly sensitive selected ion monitoring (SIM) mode matched reference mass spectra for SO_2F_2 (http://webbook.nist.gov). The identification of SO_2F_2 was confirmed by measuring an ~80 ppt SO_2F_2 mixture in zero air, which showed the same retention time and SIM mass spectra as polluted and clean ambient air (*m*/*z* abundances: 83, 100%; 102, 82%; 67, 24%; 64, 6%; 85, 5%; 48, 5%; 104, 4%; 70, 2%; and 51, 2%). Mass spectra obtained in scan mode during an SO_2F_2 ambient air pollution event also agreed with the SIM mass spectra and showed no unexpected *m*/*z* values. During routine operation, SO_2F_2 is monitored on its base *m*/*z* 83 peak, and *m*/*z* 85 is used as a qualifier ion as an additional verification of the identity of SO_2F_2 in samples and calibration standards based on a constant ratio of *m*/*z* 83 to *m*/*z* 85.

2.3. Archived Air Samples of the Northern and Southern Hemisphere

[17] To reconstruct the atmospheric history of SO_2F_2, 108 unique archived Northern Hemisphere (NH) air samples were measured at SIO, and 64 Southern Hemisphere (SH) Cape Grim air archive (CGAA) samples [*Krummel et al.*, 2007] were measured at CSIRO. Six additional SH samples were measured at SIO, of which five were in good agreement with the SH samples of similar age measured at CSIRO (ΔSO_2F_2 = 0–0.04 ppt, Δt = 3–30 days). One sample was rejected as an outlier with lower than expected SO_2F_2 mixing ratios. Similarly, four additional NH samples were measured at CSIRO, of which three were in good agreement with NH samples of the same age measured at SIO (ΔSO_2F_2 = 0.02–0.03 ppt, Δt = 0–12 days). One sample was rejected as an outlier with higher than expected SO_2F_2 mixing ratios. These tests directly show that measurements at the two sites are in agreement. On the basis of greater than two sigma deviations from of a fit through all 70 (64 at CSIRO and 6 at SIO) SH samples, four samples with lower than expected SO_2F_2 mixing ratios were rejected, and one sample with higher than expected mixing ratios was rejected, leaving 65 SH samples (93%). The 112 (108 at SIO and 4 at CSIRO) unique NH samples were collected from several sources, mainly the C. D. Keeling, R. F. Keeling, and R. F. Weiss laboratories at SIO, the Global Monitoring Division (GMD) at the National Oceanic and Atmospheric Administration (NOAA) in Boulder, and the Norwegian Institute for Air Research (NILU) in Oslo, Norway. They were filled mostly during baseline conditions, but with different techniques and for different purposes and in different types of tanks. Thirty-three NH samples showed SO_2F_2 mixing ratios below the detection limit, perhaps due to removal of SO_2F_2 on drying agents during the filling process, and 10 NH samples showed very high mixing ratios, perhaps due to sampling during an SO_2F_2 pollution event or due to accumulation and breakthrough of SO_2F_2 on drying agents used during the filling process. From the 112 unique NH samples, all 33 samples with mixing ratios below the detection limit were rejected, and 28 samples were recursively rejected as being outside of two sigma deviations from of a fit through all the NH data. Before 1999 the uncertainties of the resulting NH fits were so large that they were not suitable for the modeling and all NH data before 1999 were rejected, leaving 51 unique NH samples (46%).

3. Model Studies

3.1. Two-Dimensional 12-Box Model

[18] A flexible 2-D 12-box model has been widely used in AGAGE for inverse studies of gases with lifetimes longer than interhemispheric exchange times [e.g., *Prinn et al.*, 2005; *Xiao et al.*, 2007]. For this purpose, the model provides semihemispheric average concentrations, and accuracy in inverse problems, that are remarkably similar to those in observationally driven 3-D models [*Bousquet et al.*, 2005; *Prinn et al.*, 2005]. Its computational efficiency and flexibility enables explicit estimation of uncertainties due to

modeling and other errors. The AGAGE measurement sites have been specifically chosen to be representative of the four equal-mass semihemispheres in the lower troposphere, which are the four lowest boxes of the 2-D model. The model has horizontal divisions at 90°N, 30°N, 0°N, 30°S, and 90°S and vertical divisions at 1000, 500, 200, and 0 hPa. The model thus contains eight tropospheric boxes and four stratospheric boxes. Tests with a high-resolution 3-D model with interannually varying and observationally constrained meteorology confirm that the monthly mean mixing ratios and standard deviations at a particular AGAGE station define well the large volume averages corresponding to our 2-D model for gases whose lifetimes are much longer than the approximately few-month-long mixing times in a given semihemisphere [*Prinn et al.*, 2005]. The numeration of the boxes from north to south is: 1, 3, 5, and 7 for the lower troposphere (NH extra tropics, NH tropics, SH tropics, and SH extra tropics); 2, 4, 6, and 8 for the upper troposphere; and 9, 10, 11, and 12 for the stratosphere. The equation governing the mixing ratio χ_i of SO_2F_2 in each box i is given by

$$\frac{\partial \chi_i}{\partial t} = \frac{qP_i}{M_i} + T_i - \frac{\chi_i}{\tau_{surface,i}} - \frac{\chi_i}{\tau_{OH,i}}, \text{ for } i = 1, 3, 5, \text{and } 7, \quad (1)$$

$$\frac{\partial \chi_i}{\partial t} = T_i - \frac{\chi_i}{\tau_{OH,i}}, \text{ for } i = 2, 4, 6, \text{and } 8, \quad (2)$$

$$\frac{\partial \chi_i}{\partial t} = T_i - \frac{\chi_i}{\tau_{strat,i}}, \text{ for } i = 9, 10, 11, \text{and } 12. \quad (3)$$

[19] Here P_i is the emission rate (or source strength) of SO_2F_2 in box i, M_i is the total air mass in box i, q is the molecular weight ratio of SO_2F_2 to air, and T_i is the net convergence of the flux of SO_2F_2 into the box parameterized by using time-varying zonally averaged velocities and eddy diffusion coefficients (details given by *Cunnold et al.* [1983, 1994]). These parameters are based on observed circulation rates and have been tuned for the model to optimally predict the observed distributions of long-lived species. Thus the model is especially suitable for simulations of long-lived gases whose lifetimes much exceed interbox transport times. SO_2F_2, with a lifetime of decades (see sections 3.2, 3.3, 3.4, and 4.3), easily satisfies this requirement.

3.2. Gas Phase Loss Processes in the Troposphere

[20] The SO_2F_2 lifetime in the troposphere results from possible reactions with OH, Cl, and O_3. The lifetime due to reaction with OH in the eight tropospheric boxes is $\tau_{OH,i}$. In a collaborative effort with us, *Papadimitriou et al.* [2008] determined the upper limit of the OH rate constant $k_{OH+SO_2F_2} < 1.0 \cdot 10^{-16}$ cm^{-3} molecule^{-1} s^{-1}, which is used as a priori initial estimate in the inversion. The resulting global tropospheric lifetime τ_{OH} is at least >300 years. *Papadimitriou et al.* [2008] also determined that the reaction with Cl atoms is negligible, as the corresponding global tropospheric lifetime is >10,000 years. SO_2F_2 reacts with O_3 in the troposphere even more slowly than with OH or Cl according to *Dillon et al.* [2008], who calculated a corresponding global tropospheric lifetime of >24,000 years. Thus, tropospheric destruction of SO_2F_2 due to reactions with O_3 and Cl is negligible, and destruction due to reaction with OH is at most marginally important.

3.3. Loss Processes in the Stratosphere

[21] SO_2F_2 destruction in the stratosphere results from photolysis and reaction with $O(^1D)$. The lifetime in the four stratospheric boxes is $\tau_{strat,i}$. *Dillon et al.* [2008] suggest long stratospheric lifetimes on the basis of their measurements of the reaction of SO_2F_2 with $O(^1D)$ and UV absorption cross sections from *Pradayrol et al.* [1996] and comparisons with N_2O. *Papadimitriou et al.* [2008] calculate lifetimes with respect to reaction with $O(^1D)$ and UV photolysis of 700 years and >4700 years, respectively, and report a combined stratospheric lifetime of 630 years on the basis of a rigorous calculation with a 2-D model. The total global stratospheric lifetime used here is therefore 630 years. The latitudinal distributions of the stratospheric destruction are assumed to be the same as for N_2O, which also has a long lifetime with respect to stratospheric destruction.

3.4. Dissolution and Hydrolysis of Tropospheric SO_2F_2 in the Oceanic Mixed Layer

[22] At the baseline station Mace Head, Ireland, we found no indication of loss of SO_2F_2 in the continental boundary during stagnant meteorological conditions, and *Dillon et al.* [2008] concluded that uptake of SO_2F_2 on aerosols is not important. However, the ocean's upper mixed layer, which is on the order of 100 m thick, is turbulently mixed on a short enough timescale that it can be considered well-mixed with respect to gas exchange. For decades, oceanographers have modeled air-sea exchange of slightly soluble gases such as SO_2F_2 as being controlled by wind speed−dependent diffusion in the surface boundary layer between atmosphere and ocean, with rapid mixing within the mixed layer below [*Broecker and Peng*, 1974; *Wanninkhof*, 1992]. Factoring in the fast hydrolysis of SO_2F_2 under oceanic pH (see below) [*Cady and Misra*, 1974; *Holleman and Wiberg*, 1985], it is likely that dissolution followed by hydrolysis in the basic ocean upper mixed layer, which covers 71% of the planet, is an important factor controlling the lifetime of SO_2F_2. In contrast, hydrolysis in acidic environments such as most precipitation [*Whelpdale and Miller*, 1989; *Seinfeld and Pandis*, 1997], many lakes and rivers, and cloud water droplets is slow [*Cady and Misra*, 1974; *Holleman and Wiberg*, 1985] and likely unimportant.

[23] On the basis of the solubility and hydrolysis data of *Cady and Misra* [1974] it can be estimated that the hydrolysis of SO_2F_2 in basic waters occurs in minutes to hours (Tables 1 and 2), while the lifetime of dissolved slightly soluble gases with respect to exchange with the atmosphere is on the order of 1 month [*Broecker and Peng*, 1974]. Even in the unlikely event that the hydrolysis of SO_2F_2 is 5 times slower than measured by *Cady and Misra* [1974], SO_2F_2 would still hydrolyze within a few hours to a day, so that all SO_2F_2 entering the ocean will be hydrolyzed much more rapidly than it can exchange back with the atmosphere. Thus the transfer velocity across the air-sea boundary layer is the rate limiting step and the modeling of

Table 1. Solubility Coefficients of SO_2F_2 in Water and Seawater

°C	Bunsen Water[a]	Ostwald[b] (L) Water	Ostwald[b] (L) Seawater[d]	H_i Seawater[c] (1/L)
23.3	0.215	0.233	0.191	5.24
20	0.244	0.262[e]	0.215	4.65
15	0.296	0.313[e]	0.256	3.91
0	0.529	0.529	0.434	2.30

[a]*Cady and Misra* [1974]. The Bunsen solubility coefficient, β, is the volume (STP) of gas dissolved per unit volume of water at a gas partial pressure of 1 atm.

[b]Ostwald solubility coefficient $L = \beta$ (T[K])/273.15 K.

[c]Henry's Law constant H = 1/L.

[d]Decreased by 18% versus fresh water for the salting-out effect of sea salt for a mean salinity of 35 PSU, taken from the salting-out of N_2O in seawater [*Weiss and Price*, 1980].

[e]Based on natural logarithmic interpolation: $\ln(L) = m \cdot t + b$, t [°C], m [1/°C].

the atmospheric lifetime is highly insensitive to the oceanic hydrolysis lifetime. This makes a rough estimate of the lifetime of SO_2F_2 with respect to dissolution and hydrolysis in the ocean, τ_{ocean}, possible. On the basis of an oceanic transfer velocity, v, of 3.2–4.25 m/d (Table 3), a scale height of the troposphere, Z, of ~7000 m, a volume ratio Henry's Law coefficient, H, of 5.24–3.91 mL/mL (Table 1), and the fraction of Earth's surface area covered by ocean f_{ocean} of 0.708, the e-folding time, τ_{ocean}, of SO_2F_2 can be estimated using

$$\tau_{ocean} = \frac{Z \cdot H}{f_{ocean} \cdot v}, \tag{4}$$

with error propagation of the uncertainty ranges of v and H, to be 35 ± 14 years. This is much shorter than the lifetimes due to the tropospheric and stratospheric loss processes discussed in sections 3.2 and 3.3, indicating that dissolution and hydrolysis in the ocean surface is in fact the most important loss process for SO_2F_2. It should be stressed that *Dillon et al.* [2008] did not include this classical representation of the air-sea exchange process and oceanic mixed layer hydrolysis in their treatment of this problem and therefore obtained a very much lower estimate of the oceanic SO_2F_2 destruction rate.

[24] In our 12-box model, air-sea exchange of SO_2F_2 is described using conventional oceanic uptake calculations following the method outlined above [*Broecker and Peng*, 1974; *Wanninkhof*, 1992]. The oceanic fluxes ϕ and the corresponding lifetimes $\tau_{ocean,i}$ (which replaces $\tau_{surface,i}$ in equation (1)) due to the oceanic destruction in the lowest four boxes are calculated on the basis of the following equations:

$$\phi = \frac{v_i}{H_i}[SO_2F_2]_{air,i}\left(1 - \frac{v_i \cdot \tau_{hydro,i}}{Z_{ocean,i}}\right) \tag{5}$$

$$\tau_{ocean,i} = \frac{Z_{air,i} \cdot H_i}{f_{ocean,i} \cdot v_i\left\{1 - \frac{v_i \cdot \tau_{hydro,i}}{Z_{ocean,i}}\right\}}. \tag{6}$$

For each lower tropospheric box i = 1, 3, 5, and 7, v_i is the gas transfer or "piston" velocity which is estimated optimally in the inversion, H_i is the volume ratio Henry's Law coefficient [*Cady and Misra*, 1974] (Table 1), $\tau_{hydro,i}$ is the SO_2F_2 oceanic hydrolysis lifetime calculated from the rate constant given by *Cady and Misra* [1974] (Table 2), $f_{ocean,i}$ is the fraction of planetary surface area covered by ocean, $Z_{ocean,i}$ is the ocean mixed layer depth, $Z_{air,i}$ is the atmospheric height, and $[SO_2F_2]_{air,i}$ is the atmospheric molar concentration. The a priori initial estimates of these parameters for the model are listed in Table 3. The role of exchange of SO_2F_2 between the ocean mixed layer and the deep ocean is negligible on the timescales of interest here considering the relatively rapid rate of SO_2F_2 hydrolysis in the mixed layer, and is therefore not included in the calculation.

3.5. Inversion Approach for SO_2F_2

[25] To solve the inverse problem of deducing the sources or sinks of SO_2F_2 from the observed concentrations, a discrete recursive weighted least squares Kalman filter is used in the 12-box model. This approach has been used in a number of studies to estimate the atmospheric lifetimes or global sources of trace gases [*Prinn et al.*, 2000; *Prinn*, 2000]. The 12-box model SO_2F_2 reference case, covering the period 1942–2007.96, is described in section 4.2. The AGAGE SO_2F_2 measurements began in 1978, which allows sufficient model spin-up time.

[26] In the Kalman filter, the state vector contains eight factors which are optimally estimated during the inversion: F_{ocean}, F_{OH}, and six emission coefficients f_i. The basic approach for the SO_2F_2 sink and source estimation is to multiply the reference inverse oceanic lifetime $1/\tau_{ocean,i}$ and the tropospheric lifetime $1/\tau_{OH,i}$ (see sections 3.4 and 3.2) by the dimensionless factors F_{ocean} and F_{OH}. Because of the fast hydrolysis (i.e., short hydrolysis lifetime $\tau_{hydro,i}$), F_{ocean} is approximately proportional to the transfer velocity v_i (see equations (4) and (6)). F_{OH} is proportional to the reaction rate constant $k_{OH+SO_2F_2}$. The total global emissions in the model are essentially determined by the six emission coefficients f_i and described with the emission function

$$E(x) = f_0 + f_1 NP_1(x) + \frac{f_2}{3}N^2P_2(x) + f_3 NP_3(x) + \frac{f_4}{10}N^2P_4(x) + f_5 NP_5(x) \tag{7}$$

$$E(x)\ \left[\frac{\text{Gg}}{\text{yr}}\right], N = \frac{t_{end} - t_0}{2}[\text{years}], x = \frac{t - t_0}{N} - 1,$$

where $P_n(x)$ is the Legendre polynomial of the order n, with its argument normalized to N and measured from the midpoint of the $2N$ yearlong interval from t_0 = 1960 to t_{end} = 2007.96. Likely latitudinal distributions of emissions are assessed on the basis of available industrial data as discussed in section 4.3.

[27] To avoid inconsistencies during the inversion, regular monthly means of the observed mixing ratios are needed as input data. However, only sparse data are available before in situ measurements began. Therefore polynomial functions

$$x(t) = p_0 + p_1 t + p_2 t^2 + p_3 t^3\ [\text{ppt}] \tag{8}$$

Table 2. Hydrolysis Lifetimes $\tau_{hydro,i}$ of SO_2F_2 in the Ocean Surface Mixed Layer

Region	Average Annual Temperature[a] (°C)	Average Annual pH[b]	τ_{hydro}[c] (days)
Tropics (0°–30°N/0°–30°S)	23–29	8.05–8.01	0.017–0.029
Extratropics (30°N–90°N/30°S–90°S)	−2–23	8.1–8.3	0.023–0.203

[a]Annual average temperatures from *Locarnini et al.* [2006].
[b]Annual average pH from *Orr et al.* [2005].
[c]According to *Cady and Misra* [1974] at pH $\geq$ 7.5 and 0°C to 25°C the rate constant for hydrolysis of SO_2F_2 in water $k_{hydro} = a \cdot \exp(-E \cdot (R \cdot T)^{-1}) \cdot [OH^-]$ in $[s^{-1}]$ with the preexponential coefficient $a = 1.67 \cdot 10^{12}$ L · mol^{-1} · s^{-1}, the activation energy for hydrolysis of SO_2F_2 by the hydroxyl ion in basic water E = 13,100 cal · mol^{-1} (or 54,847 J · mol^{-1}), the gas constant R = 1.9859 cal · mol^{-1} · K^{-1} (or 8.3145 J · mol^{-1} · K^{-1}), the average temperature of ocean mixed layer T (K), and the average hydroxyl ion concentration of the ocean mixed layer $[OH^-] = 10^{-(14-pH)}$ (mol/L). Hydrolysis lifetime $\tau_{hydro} = 1/k_{hydro}$.

with t in years were fitted to the observational data and used as model input. For the SH extratropics (30°S–90°S, box 7) the SH CGAA tank data (section 2.3) and the background monthly mean in situ values with pollution events removed for Cape Grim, Tasmania were combined. Similarly, for the NH extra tropics (30°N–90°N, box 1) the NH tank data (section 2.3) and the background monthly mean in situ values with pollution events removed for Trinidad Head, California, and Mace Head, Ireland, were combined. The NH tropics (0°–30°N, box 3) contain Ragged Point, Barbados, data and the SH tropics (0°–30°S, box 5) contain Cape Matatula, American Samoa, data. Coefficients p_i for the polynomial fits are listed in Table 4. The derived atmospheric histories for the SH and NH are discussed in section 4.2. Uncertainties of each polynomial fit were calculated as the root sum square of the measurement standard deviations and the deviations of the measurements from the polynomial fit for periods with similar deviations. These uncertainties are compared to the differences between the measurements and the model to assess the quality of the inversions in section 4.3. Only monthly mean in situ data until May 2007 are used, since later in situ data are referenced against working standards which were still in use at the field stations and had thus not been returned to SIO for recalibration.

[28] Owing to the semilinear nature of the inversion problem, several iterations of the filtering runs are needed. The iteration ends when the final estimates of the state vector converge with the initial estimate from that particular filtering run. For every inversion iteration, 100% error was assigned to the initial estimate of each factor F_{ocean}, F_{OH}, and f_i. In addition to the measurement errors, we also included errors resulting from transport uncertainties in the inversion results discussed below.

4. Results and Discussion

4.1. Observations

[29] At the Mace Head, Ireland, and Cape Grim, Tasmania, AGAGE remote stations, baseline conditions are generally observed with mean mixing ratios for January 2007 of ~1.53 ppt at Mace Head and ~1.35 ppt at Cape Grim (Figure 1). Sporadic pollution events have been observed at Mace Head, pointing to small local or regional emissions.

[30] No pollution events above background were observed at Cape Grim (Figure 1), Cape Matatula, American Samoa (not shown), and at urban Aspendale, Australia (38°S, 145°E, preliminary data), during the period of the study. The first above-baseline events were observed at Cape Grim and Aspendale in mid-2008 after SO_2F_2 was registered for use in Australia (M. Krieger, Dow AgroSciences, personal communication, 2008). Australian regulatory agencies are not aware of any use prior to 2008 (P. J. Fraser, CSIRO, personal communication, 2008). SO_2F_2 has not yet been registered for use in other Southern Hemisphere countries and we are not aware of any sales in that region (M. Krieger, Dow AgroSciences, personal communication, 2008). We conclude therefore that SO_2F_2 has been used almost entirely in the NH.

[31] At Trinidad Head on the Northern California coast, background conditions similar to Mace Head are observed when air originates offshore or from colder areas of Northern California, while SO_2F_2 pollution events are generally associated with air originating from Southern California where fumigation with SO_2F_2 for termite control is common (air history maps demonstrating this were provided by the UK Met Office using the NAME 3-D Lagrangian dispersion model [*Manning et al.*, 2003; *Jones et al.*, 2007]). In urban La Jolla on the Southern California coast, several hundred to several thousand ppt are frequently observed owing to

Table 3. Initial Estimates of Oceanic Transfer Velocity v_i, Henry's Law Coefficient H_i, Oceanic Hydrolysis Lifetime $\tau_{hydro,i}$, Fraction of Total Surface Area Covered by Ocean $f_{ocean,i}$, Atmospheric Box Height $Z_{air,i}$, and Ocean Mixed Layer Depth $Z_{ocean,i}$ for Each Lower Troposphere Box

Parameter	30°N–90°N	0°–30°N	0°–30°S	30°S–90°S
v_i[a] (m/d)	4.00	3.22	3.20	4.25
H_i[b]	3.906	5.236	5.236	3.906
$\tau_{hydro,i}$[c] (days)	0.042	0.021	0.021	0.042
$f_{ocean,i}$[d]	0.504	0.711	0.770	0.850
$Z_{ocean,i}$[e] (m)	150	50	50	100
$Z_{air,i}$[f] (m)	5495.5	5799.68	5799.68	5495.5

[a]Oceanic transfer velocities $v_i = 0.31\ (660/Sc)^{0.5}\ U_{10}^2$ for SO_2F_2 were estimated for each lower tropospheric box using area, sea surface temperature (SST), and Schmidt number (Sc) data from the *Takahashi et al.* [2002b] carbon dioxide climatology (on a 4° × 5° grid) and QSCAT winds for 1999–2004 (U_{10}) over the ocean, assuming that the diffusion coefficient of SO_2F_2 in seawater is ~40% less than that of carbon dioxide. The estimated absolute uncertainty for each v_i is ~50% to reflect differences among the various parameterizations for v_i with wind speed. The estimated uncertainty for the ratios of v_i/v_j for any two boxes i and j is ~20%. That is, the relative latitudinal distribution of v_i is better constrained than each v_i (R. Wanninkhof, personal communication, 2008).
[b]Volume ratio Henry's Law coefficient H_i = 1/(Ostwald coefficient); see Table 1.
[c]The oceanic hydrolysis lifetime $\tau_{hydro,i}$ is calculated in Table 2.
[d]Land and ocean fractions from NASA Goddard Institute for Space Studies (http://data.giss.nasa.gov/landuse/soilunit.html).
[e]Climatology oceanic mixed layer depth from National Center for Environmental Prediction (http://www.cpc.ncep.noaa.gov/cgi-bin/godas_parameter.pl).
[f]The 1000- to 500-hPa atmospheric height is calculated using 287 · T/9.81 · log (1000/5000), where T is the temperature in each box.

Table 4. Parameters of Polynomial Fits of Observational Data Used as Model Input

Location	Time Period	p_0 (ppt)	p_1 (ppt/a)	p_2 (ppt/a^2)	p_3 (ppt/a^3)	R^2
NH extratropics (30°N–90°N)[a]	April 1999 to May 2007	5671.025	−5.718352	1.441698E-3	0	0.966
NH tropics (0°–30°N)[b]	July 2005 to May 2007	−151,376.92	150.831330	−0.037571545	0	0.758
SH tropics (0°–30°S)[c]	June 2006 to May 2007	−149,513.42	148.936658	−0.037090176	0	0.883
SH extratropics (30°S–90°S)[d]	April 1978 to May 2007	−66,048.78	100.721066	−0.051206630	8.679269E-06	0.996

[a]Northern Hemisphere (NH) tank data and background monthly mean in situ values for Trinidad Head, California and Mace Head, Ireland.
[b]Background monthly mean in situ values for Ragged Point, Barbados.
[c]Background monthly mean in situ values for Cape Matatula, American Samoa.
[d]Southern Hemisphere (SH) tank data (Cape Grim air archive) and background monthly mean in situ values for Cape Grim, Tasmania.

nearby fumigation with SO_2F_2, but the lowest observed values agree well with the baseline Mace Head and Trinidad Head records. Preliminary results from the new AGAGE-affiliated station at Gosan, Jeju Island, Korea (33°N, 126°E) operated by Seoul National University show frequent pollution events (not shown), pointing to SO_2F_2 sources in eastern Asia, in agreement with the presence of Chinese SO_2F_2 production and emissions.

4.2. Reconstruction of the Atmospheric History of SO_2F_2

[32] The atmospheric history of SO_2F_2 in the SH was reconstructed from analysis of archived SH air from the Cape Grim air archive (CGAA) [*Krummel et al.*, 2007] (section 2.3) and background monthly mean in situ for Cape Grim, Tasmania. SO_2F_2 mixing ratios in Antarctic firn air samples measured in our laboratory (J. E. Shields, unpublished data, 2008) agree well with our recent SH measurements at the top of the firn profile and showed no detectable SO_2F_2 at the bottom of the profile which predate industrial SO_2F_2 production. We therefore assume that there is negligible natural SO_2F_2 in the atmosphere and that the history of SO_2F_2 in the atmosphere began with the onset of its industrial production in 1960 (see section 4.3). The atmospheric history of SO_2F_2 in the NH was reconstructed from analysis of archived NH air and background monthly mean in situ values for Mace Head, Ireland, and Trinidad Head, California. In contrast to the SH tanks, the NH tanks were collected from various sources and show a larger scatter in SO_2F_2 and other trace gases as discussed in section 2.3. Nevertheless, after filtering of outliers, a clear atmospheric trend from 1999 to 2007 was obtained for the NH. The excellent quality of the CGAA enabled the reconstruction of the atmospheric trend from 1978 to 2007 for the SH. The resulting measured SO_2F_2 values and fitted baseline trends for both hemispheres are plotted in Figure 2. SO_2F_2 has been accumulating in the global atmosphere with a growth rate of 5 ± 1% per year since 1978 and the interhemispheric concentration ratio has been 1.13 ± 0.02 over the 1999–2007 period.

4.3. Emission and Lifetime Estimates

[33] Since no significant pollution events were observed at either SH AGAGE station (SO_2F_2 was not registered for fumigation use in Australia or other Southern Hemisphere countries prior to 2008), and since we found no other evidence of SO_2F_2 use in the SH (see section 4.1), we assumed that all emissions have been in the NH. To account for possible emissions in Hawaii (M. Krieger, Dow AgroSciences, personal communication, 2008), two emission

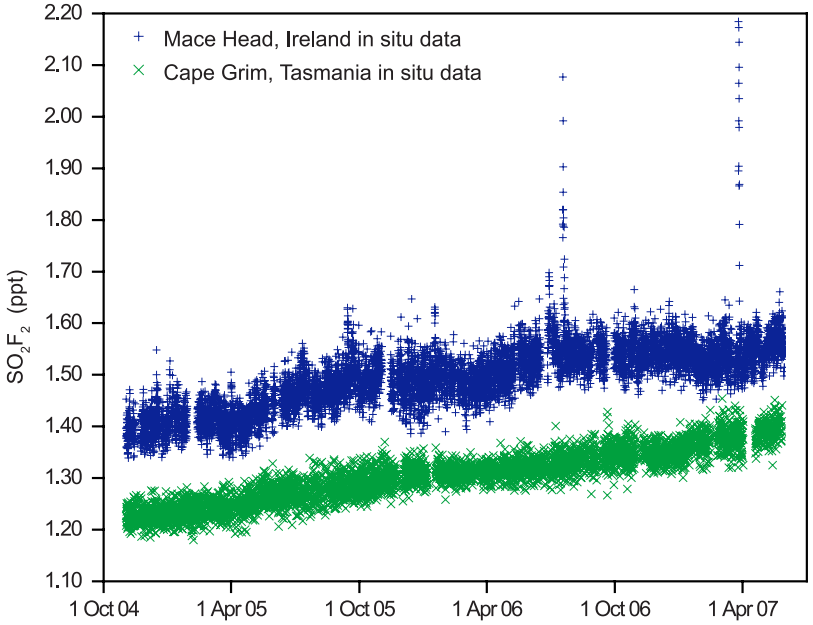

Figure 1. In situ observations of SO_2F_2 at Mace Head, Ireland, and Cape Grim, Tasmania. Sporadic pollution events have been observed at Mace Head, Ireland, pointing to local or regional emissions. No pollution events were observed at Cape Grim, Tasmania, and Cape Matatula, American Samoa (not shown), indicating that SO_2F_2 has as of yet mostly been used in the Northern Hemisphere.

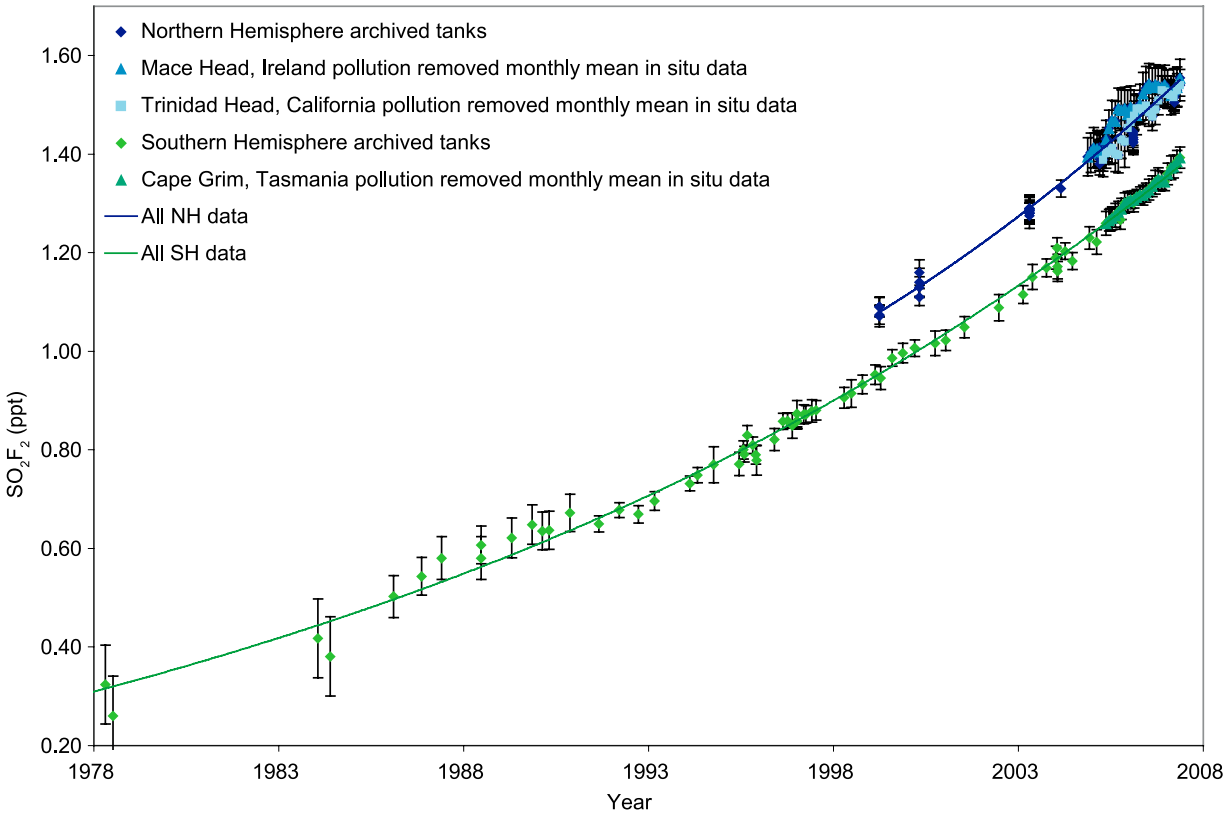

Figure 2. Atmospheric history of SO_2F_2 in the Northern Hemisphere (NH) and Southern Hemisphere (SH). NH trends were reconstructed from 1999 to 2007 from archived NH air (dark blue diamonds), background monthly mean in situ values for Mace Head, Ireland (blue triangles), and Trinidad Head, California (light blue squares). SH trends were reconstructed from 1978 to 2007 from archived SH air (Cape Grim Air Archive, green diamonds) and background monthly mean in situ values for Cape Grim, Tasmania (dark green triangles). Polynomial fits to NH (blue line) and SH data (green line) are shown. Growth rates of 5 ± 1% per year were observed. The interhemispheric concentration ratio has been 1.13 ± 0.02 over the 1999–2007 period.

scenarios were investigated. Scenario a assumes 100% of the emissions in the NH extratropics (30°N–90°N) and scenario b assumes 90% of the emissions in the NH extratropics (30°N–90°N) and 10% in the NH tropics (0°–30°N).

[34] The quality of the inversions can be assessed by comparing the residual differences between the measurements and the model to the uncertainties of the polynomial fits to the measurements (see section 3.5). As seen in Figure 3 for scenario a the residuals are small (<0.02 ppt), randomly distributed around zero, and within the uncertainties of the polynomial measurement fits for the NH extratropics (30°N–90°N), the NH tropics (Cape Matatula, American Samoa, 0°–30°S), and the SH extra tropics (Cape Grim, Tasmania, 30°S–90°S), which reflects a good inversion as the time averaged state vector is estimated. The residuals for scenario b (not shown) are very similar. For the NH tropics (Ragged Point, Barbados, 0°–30°N) the residuals are larger and mostly positive, albeit still within the uncertainties of the polynomial measurement fits, except for a short period in late 2006. This could be related to the shifting of the intertropical convergence zone (ITCZ) which complicates the inversion for Ragged Point. Inversions of other species have resulted in similar differences for Ragged Point as the complex meteorology which would be needed to fully describe the observations at Barbados is not included. Also, the fit of the Ragged Point data has the lowest correlation coefficient (R^2 = 0.758; see Table 4) reflecting that the fit smoothed out some of the observed variability in the record.

[35] During the inversions of the SO_2F_2 observations, the dimensionless factors F_{ocean} (proportional to the inverse oceanic lifetimes $1/\tau_{ocean,i}$) and F_{OH} (proportional to the inverse tropospheric lifetimes owing to reaction with the OH radical $1/\tau_{OH,i}$) and the six coefficients f_i (describing the emission function) were estimated optimally to best explain the observations. The results are shown in Tables 5 and 6. The final estimates (last iteration) and the error reduction from the first iteration do not differ significantly between emission Scenarios a and b, showing that we cannot distinguish between these two scenarios.

[36] The resulting modeled F_{ocean} = 1.3–1.4 with an error of ~30%. Owing to the fast hydrolysis of SO_2F_2, F_{ocean} is approximately proportional to the transfer velocity v_i (see equation (6)). The estimated uncertainty of the a priori initial v_i (and thus F_{ocean}) is ~50% (R. Wanninkhof, personal communication, 2008) to reflect differences among various parameterizations of air-sea exchange rates with

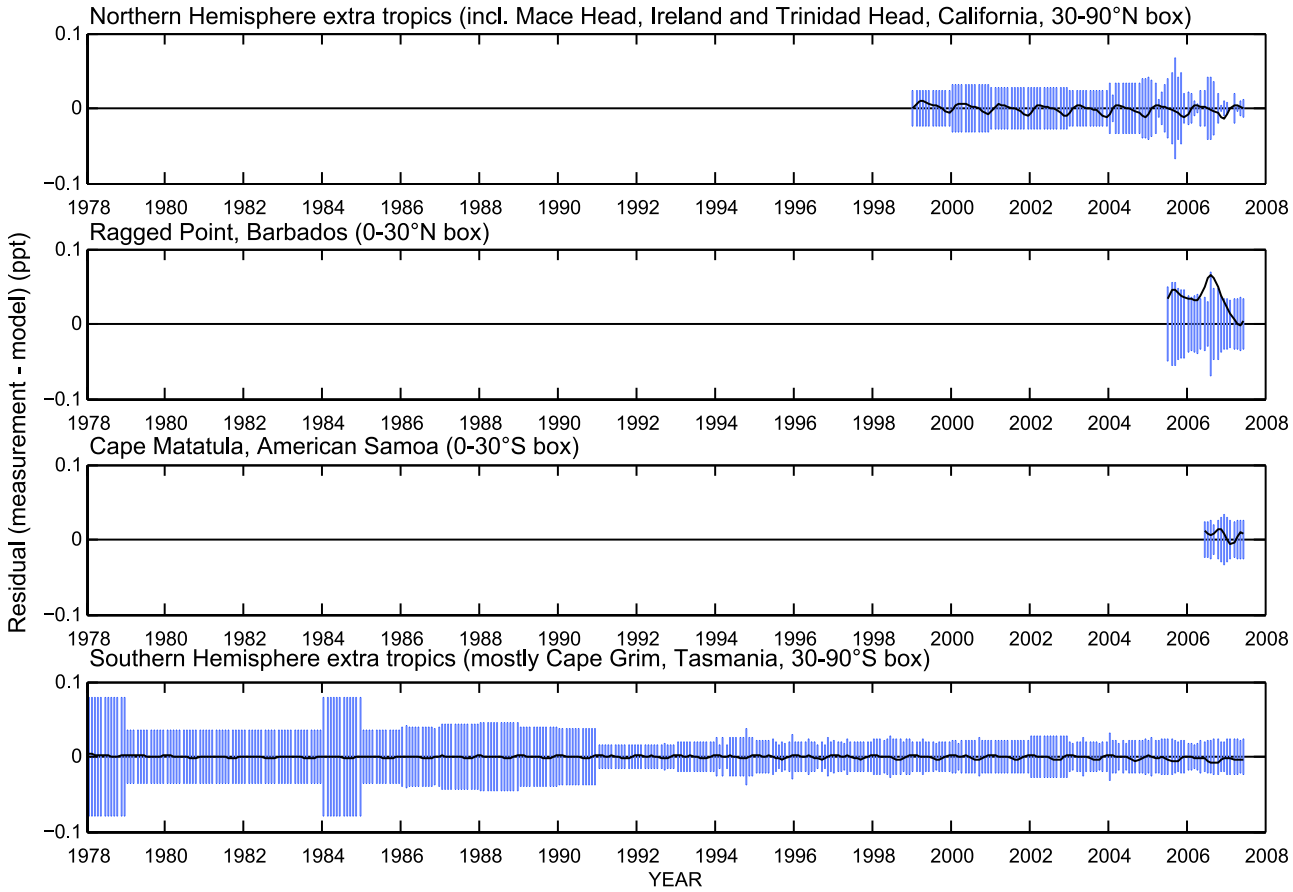

Figure 3. Residuals between the polynomial measurement fits and the 12-box model calculations from the inversion for emission scenario a (100% in 30°N–90°N box). Residuals (black) are small (<0.02 ppt), randomly distributed around zero, and within the uncertainties of the polynomial measurement fits (blue; see section 3.5) for the 30°N–90°N box, the 0°–30°S box, and the 30°S–90°S box. For the 0°–30°N box the residuals are larger and mostly positive, albeit mostly still within the uncertainties of the polynomial measurement fits.

wind speed. The 30–40% deviation of the inverted F_{ocean} from unity represents reasonable agreement within the expected uncertainty of ~50%. A different parameterization with higher (lower) values of v_i will result in a lower (higher) F_{ocean}, but the inversion results are similar, as long as the relative latitudinal distribution of v_i is similar. Note that the estimated uncertainty for the ratios of v_i/v_j for any two boxes i and j is ~20%. That is, the relative latitudinal distribution of v_i is better constrained than each v_i (R. Wanninkhof, personal communication, 2008). We have verified that perturbations of the latitudinal distribution of v_i by 20% have no significant effect on the inversion results.

[37] The modeled F_{OH} = 0.2–0.3 with an error of more than 100%, which means that the inversion is insensitive to the OH sink.

[38] The resulting average total global lifetime for both inversions τ^G_{total} = 36 ± 11 years (Table 7). The average atmospheric lifetime for oceanic loss τ^G_{ocean} = 40 ± 13 years and the average atmospheric lifetime due to reaction with OH τ^G_{OH} = 1604–999 years (with more than 100% error) assuming a stratospheric lifetime $\tau^G_{stratos}$ = 630 years based on our collaborative work with *Papadimitriou et al.* [2008]. This confirms that hydrolysis of SO_2F_2 in the oceanic mixed layer is the overwhelmingly dominant global sink and that reaction with OH is unimportant. This also explains why the error of F_{OH} (and τ^G_{OH}) could not be reduced during the inversion. The agreement between the inversion result of τ^G_{ocean} = 40 ± 13 years, which is based on a full air-sea exchange description, and the rough estimate of τ_{ocean} =

Table 5. Dimensionless Factors for Transfer Velocity, OH Reaction, and Legendre Coefficients for the Emission Function for the First and Last Iteration of the Inversion for Scenario a With 100% of the Emissions in the 30°N–90°N Box[a]

	First Iteration		Last Iteration			
	1942	Error, %	2007.96	Error,[b] %		Error Reduction, %
F_{ocean}	1.0	100	1.30	0.40	31	69
F_{OH}	1.0	100	0.21	0.39	>100	
f_0	1.385	100	0.820	0.078	9	91
f_1	0.05771	100	0.0324	0.0041	13	87
f_2	0.0	100	0.0011	0.0002	18	82
f_3	0.0	100	0.0056	0.0006	11	89
f_4	0.0	100	−0.0013	0.0003	24	76
f_5	0.0	100	0.0021	0.0014	62	38

[a]Transfer velocity, F_{ocean}; OH reaction, F_{OH}; Legendre coefficients, f_i.
[b]The listed errors include modeling errors determined by sensitivity studies.

Table 6. Dimensionless Factors for Transfer Velocity, OH Reaction, and Legendre Coefficients for the Emission Function for the First and Last Iteration of the Inversion for Scenario b With 90% of the Emissions in the 30°N–90°N Box and 10% in the 0°–30°N Box[a]

	First Iteration		Last Iteration			
	1942	Error, %	2007.96	Error[b]		Error Reduction, %
F_{ocean}	1.0	100	1.41	0.42	30%	70
F_{OH}	1.0	100	0.32	0.39	>100%	
f_0	1.385	100	0.843	0.082	10%	90
f_1	0.05771	100	0.0336	0.0044	13%	87
f_2	0	100	0.0012	0.0002	17%	83
f_3	0	100	0.0057	0.0006	11%	89
f_4	0	100	−0.0013	0.0003	24%	76
f_5	0	100	0.0022	0.0013	59%	41

[a]Transfer velocity, F_{ocean}; OH reaction, F_{OH}; Legendre coefficients, f_i.
[b]The listed errors include modeling errors determined by sensitivity studies.

35 ± 14 years (section 3.4), which is based on a simple oceanic uptake calculation using transfer velocity and solubility, and assumes instant hydrolysis, is striking. In contrast, as noted above, *Dillon et al.* [2008] did not consider the air-sea exchange of slightly soluble gases in their assessment of the lifetime of SO_2F_2 in the marine boundary layer.

[39] The Legendre coefficients f_i for the emission function are well defined with errors of 9–18% and error reductions of 82–91% for the first four coefficients f_0–f_3 (the importance of f_i decreases with i). The resulting global emissions for both scenarios (Figure 4) agree within the uncertainties of ∼0.14 Gg/a (shown as dotted lines). Modeled emissions rose from ∼0.6 Gg/a in 1978 to ∼1.1 Gg/a in 1995 and ∼1.9 Gg/a in 2007.

[40] Owing to the increasing fraction of total surface area covered by ocean from north to south, lifetimes tend to decrease and emission tend to increase when larger fractions of emissions are allowed to occur farther to the south. However, the two emission scenarios a and b are reasonable assumptions of the most likely latitudinal distribution based on available industrial data, which are likely to be reasonably accurate because SO_2F_2 is a highly toxic compound that is strictly regulated. If 33% of the emissions are allowed to occur in the NH tropics (0°–30°N), the resulting global lifetime of 29 years still agrees with the τ^G_{total} = 36 ± 11 years for scenarios a and b, although the resulting emissions are ∼0.1 Gg/a (1990) to ∼0.2 Gg/a (2007) higher than the emissions for scenarios a and b.

[41] For comparison to the modeled emissions, a global industrial estimate (M. Krieger, Dow AgroSciences, personal communication, 2008) and a U.S. industrial estimate (Dow AgroSciences internal production and sales data and TRI Explorer (Environmental Protection Agency, online data, 2006)) are included in Figure 4. Note that the global industrial estimate is more uncertain because production, sales, and usage data are generally trade secrets. Also note that SO_2F_2 was produced from 1960 to 1975, but detailed production data for this period are unavailable, and that stack emissions of SO_2F_2 have only been accounted for since 1995 (TRI Explorer (Environmental Protection Agency, online data, 2006)). Also shown in Figure 4 is the reported SO_2F_2 pesticide use in California based on the Pesticide Use Report (California Environmental Protection Agency online reports, 1989–2006) which represents for ∼37–56% of the global usage estimate and ∼41–75% of the U.S. usage estimate.

[42] The reported California pesticide use is 0.1–0.5 Gg/a lower than the modeled emissions and global industrial estimates are on average 1.5 ± 0.3 times the modeled emissions, that is ∼50 ± 30% higher. Discrepancies of such a magnitude between measurement based and industrial emission estimates are common for many anthropogenic atmospheric trace gases, and could be caused by accounting errors in the industrial estimate. However, because SO_2F_2 production prior to about 1997 was mostly by one company (Dow AgroSciences) which has provided their production estimate, the difference is surprising. A calibration error of such magnitude is very unlikely given the proven AGAGE calibration methods.

[43] Initial inversions of the atmospheric SO_2F_2 observations using the global industrial estimate as an initial estimate were unsuccessful in yielding a simple calibration scaling factor. Assuming that a smoothed global industrial estimate is correct (to avoid inconsistencies during the inversion caused by the fluctuations in the industrial estimate) leads to lifetimes which are not in agreement with the observed interhemispheric gradient and the release pattern. A simple calibration scaling factor cannot therefore explain the discrepancy.

[44] A delay between production and emission (stockpiling) of several years would be required to bring the industrial estimate and the modeled emissions in closer agreement, but this seems very unlikely even though some degree of stockpiling may have taken place causing the strong fluctuations in reported production values.

[45] There is no experimental evidence for a significant terrestrial sink. For example, mixing ratios do not drop at the Mace Head, Ireland, AGAGE remote station during stagnant meteorological conditions. We nevertheless carried out modeled inversions including a hypothetical terrestrial sink proportional to ice-free land surface areas as a possible explanation for the discrepancy between the global industrial estimate and the modeled emission estimates without such a land sink. If the a priori initial lifetime with respect to a hypothetical land sink is chosen to be the same as the initial oceanic sink (∼50 years), the inversion yields a negative land sink. If the initial lifetime with respect to a

Table 7. Total Global Lifetime of SO_2F_2 and Atmospheric Lifetimes for Oceanic Loss, OH Reaction, and Stratospheric Loss for Both Emission Scenarios[a]

	Lifetime (years)			
Emission Scenario	τ^G_{total}	τ^G_{ocean}	τ^G_{OH}[b]	$\tau^G_{stratos}$[c]
Scenario a	37 ± 11	41 ± 13	1604	630
Scenario b	34 ± 10	38 ± 11	999	630
Average	36 ± 11	40 ± 13		

[a]Total global lifetime of SO_2F_2, τ^G_{total}; atmospheric lifetimes: oceanic loss, τ^G_{ocean}; OH reaction, τ^G_{OH}; and stratospheric loss, $\tau^G_{stratos}$.
[b]The inversion is insensitive to the reaction of SO_2F_2 with OH and the error of τ^G_{OH} is more than 100%.
[c]The stratospheric lifetime $\tau^G_{stratos}$ has been taken from our collaborative work with *Papadimitriou et al.* [2008] and has not been estimated optimally in the inversion.

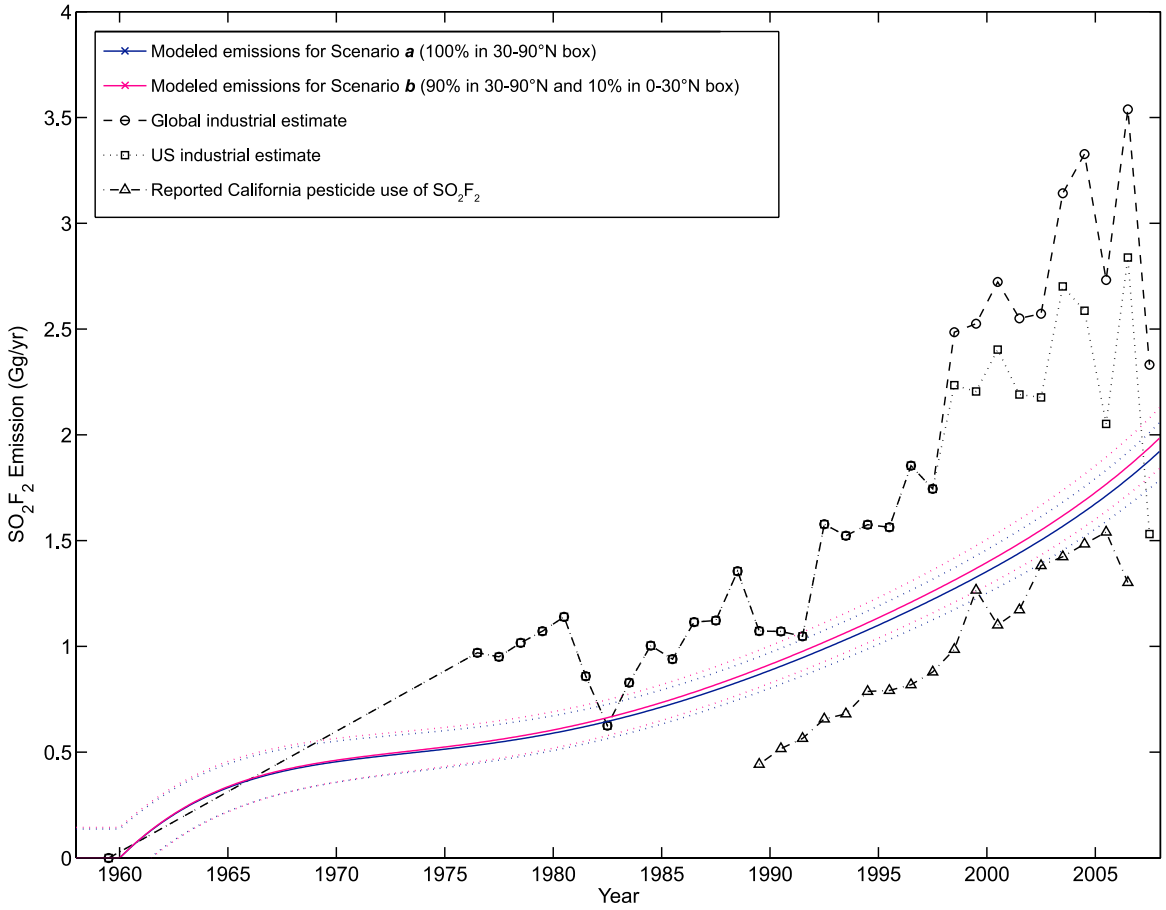

Figure 4. Modeled SO_2F_2 emissions (Gg/a) for scenarios a and b, global industrial estimate, U.S. industrial estimate, and reported pesticide use of SO_2F_2 in California. Uncertainties of the modeled global emission are indicated by dotted lines. The global industrial estimate is based on assumed global industrial activity, and the U.S. industrial estimate is based on Dow AgroSciences internal data (M. Krieger, Dow AgroSciences, personal communication, 2008) and the TRI Explorer (Environmental Protection Agency online data, 2006). SO_2F_2 was produced from 1960 to 1975, but actual data are unavailable, and stack emissions have only been accounted for since 1995. The pesticide use in California is taken from the California Pesticide Use Report (California Environmental Protection Agency online reports, 1989–2006).

hypothetical land sink is chosen to be ~100 years, the inverted global and oceanic lifetimes are the same as without a land sink (scenario a, Table 7), the lifetime with respect to the hypothetical land sink is long and undefined (~1800 years, 100% error), the lifetime with respect to the OH reactions remains long and undefined (~1260 years, 100% error), and the emissions are not statistically different from scenario a. This means that no significant land sink is allowed by the data and the model. Thus we conclude that a missing land sink is extremely unlikely to explain the observed discrepancy.

[46] Besides a yet unknown or underestimated known sink, a possible explanation is that ~1/3 of SO_2F_2 is destroyed during the fumigation process and only ~2/3 is vented to the atmosphere. Similarly large fractions of methyl bromide are known to be destroyed during fumigation [*Yagi et al.*, 1995; *Yates et al.*, 1998], although direct evidence of SO_2F_2 destruction during fumigation, such as correspondingly high residual fluoride ion, is so far lacking (M. Krieger, Dow AgroSciences, personal communication, 2008). This question should be addressed with further experimental work.

5. Conclusions

[47] The atmospheric history of SO_2F_2 in both hemispheres was reconstructed from in situ measurements and archived air, showing that SO_2F_2 has been accumulating in the global atmosphere with growth rates of 5 ± 1% per year since 1978. Mixing ratios of ~0.3 ppt (SH) in 1978, ~0.95 ppt (SH) and ~1.08 ppt (NH) in early 1999, as well as ~1.35 ppt (SH) and ~1.53 ppt (NH) in early 2007 were observed. The SO_2F_2 interhemispheric concentration ratio has been 1.13 ± 0.02 over the 1999–2007 period.

[48] Sporadic pollution events were seen at the Mace Head, Ireland, AGAGE remote station, while remote and urban Southern Hemisphere AGAGE stations (Cape Grim, Tasmania; Aspendale, Australia; and Cape Matatula, American Samoa) showed baseline conditions since the beginning of in situ measurements with no pollution events. This

indicates that SO_2F_2 has been mostly used in the NH. SO_2F_2 pollution events seen at the Trinidad Head AGAGE station on the Northern California coast are generally associated with air originating from Southern California where fumigation with SO_2F_2 is common, while background conditions similar to Mace Head are observed at other times. At urban La Jolla on the Southern California coast, several hundred to several thousand ppt of SO_2F_2 are frequently observed owing to nearby fumigation with SO_2F_2, but the lowest observed values agree well with the Mace Head and Trinidad Head baseline records.

[49] Inversions with a 2-D 12-box model lead to a global total lifetime τ^G_{total} = 36 ± 11 years for SO_2F_2 which is substantially longer than previous estimates of less than 4.5 years given in a recent European Union report on the environmental fate and behavior of SO_2F_2 [*Swedish Chemical Agency*, 2005]. Dissolution and hydrolysis in the ocean is the overwhelmingly dominant global sink with an atmospheric lifetime for oceanic loss τ^G_{ocean} = 40 ± 13 years. Other tropospheric and stratospheric sinks processes are only marginally important in agreement with kinetic studies [*Dillon et al.*, 2008; *Papadimitriou et al.*, 2008].

[50] Modeled SO_2F_2 emissions rose from ∼0.6 Gg/a in 1978 to ∼1.1 Gg/a in 1995 and ∼1.9 Gg/a in 2007. But global industrial production estimates based on assumptions about global industrial activity (M. Krieger, Dow AgroSciences, personal communication, 2008) have averaged ∼50% higher than the modeled emissions. We have attempted to model this discrepancy as being due to a hypothetical land sink that is proportional to ice-free land surface area, but the discrepancy persisted in the new inversion results. Although no confirming experimental evidence exists, we conclude that besides a yet unknown or underestimated known sink, a possible explanation is that ∼1/3 of SO_2F_2 is destroyed in the fumigation process and only ∼2/3 is vented to the atmosphere.

[51] At a mean global mixing ratios of ∼1.4 ppt, the radiative forcing of SO_2F_2 is small and SO_2F_2 is probably an insignificant source of sulfur to the stratosphere compared to carbonyl sulfide (COS) with a lifetime of 3–6 years and a mixing ratio of ∼500 ppt [*Chin and Davis*, 1995; *Kettle et al.*, 2002; *Montzka et al.*, 2007]. However, given a SO_2F_2 global warming potential similar to that of CFC-11 (∼4780, 100-year time horizon, based on measured infrared cross sections and the modeled lifetime of 36 ± 11 years *Papadimitriou et al.* [2008]) and in view of likely increases in its future use, continued atmospheric monitoring of SO_2F_2 is highly warranted.

[52] **Acknowledgments.** This work was carried out as part of the international AGAGE research program, which is supported in the United States by the Upper Atmospheric Research Program of NASA, in Australia by CSIRO and the Bureau of Meteorology, and in the UK by DEFRA and NOAA. We thank E.J. Dlugokencky, J.W. Elkins, B.D. Hall, and S.A. Montzka at NOAA/GMD; C.D. Keeling and R.F. Keeling at SIO; O. Hermansen, C. Lunder, and N. Schmidbauer at NILU; and R.C. Rhew at University of California, Berkeley, for air samples. We are grateful to D. Barnekow and M. Krieger at Dow AgroSciences for approval to obtain a sample of pure SO_2F_2 (Vikane) with which we made primary standards. We thank the anonymous reviewers for their comments and questions. We particularly thank M. Krieger for providing the global industrial SO_2F_2 emission estimates given in this paper and for his feedback. We especially thank J.B. Burkholder at NOAA/CSD for valuable discussions and collaboration on kinetic studies of SO_2F_2, R. Wanninkhof at NOAA/AOML for providing the initial estimates of the oceanic transfer velocities for the four tropospheric model boxes and for valuable input regarding the modeling of SO_2F_2 sea-air exchange, and J.E. Shields at SIO for access to her unpublished modeling of our firn air measurements. D.M. Cunnold at GaTech and P.J. Crutzen at SIO provided valuable discussions.

References

Bousquet, P., D. A. Hauglustaine, P. Peylin, C. Carouge, and P. Ciais (2005), Two decades of OH variability as inferred by an inversion of atmospheric transport and chemistry of methyl chloroform, *Atmos. Chem. Phys.*, *5*, 2635–2656.

Broecker, W. S., and T. H. Peng (1974), Gas-exchange rates between air and sea, *Tellus*, *26*(1–2), 21–35.

Cady, G. H., and S. Misra (1974), Hydrolysis of sulfuryl fluoride, *Inorg. Chem.*, *13*(4), 837–841, doi:10.1021/ic50134a016.

California Environmental Protection Agency (2005), Sulfuryl fluoride (Vikane®), risk characterization document, III, Environmental fate, final draft report, Dep. of Pestic. Regulat., Environ. Monit. Branch, Sacramento, Calif.

Chin, M., and D. D. Davis (1995), A reanalysis of carbonyl sulfide as a source of stratospheric background sulfur aerosol, *J. Geophys. Res.*, *100*(D5), 8993–9005, doi:10.1029/95JD00275.

Collett, J. L., A. Bator, X. Rao, and B. B. Demoz (1994), Acidity variations across the cloud drop size spectrum and their influence on rates of atmospheric sulfate production, *Geophys. Res. Lett.*, *21*(22), 2393–2396, doi:10.1029/94GL02480.

Crutzen, P. J. (1976), Possible importance of CSO for sulfate layer of stratosphere, *Geophys. Res. Lett.*, *3*(2), 73–76, doi:10.1029/GL003i002p00073.

Cunnold, D. M., R. G. Prinn, R. A. Rasmussen, P. G. Simmonds, F. N. Alyea, C. A. Cardelino, A. J. Crawford, P. J. Fraser, and R. D. Rosen (1983), The Atmospheric Lifetime Experiment: 3. Lifetime methodology and application to 3 years of $CFCl_3$ data, *J. Geophys. Res.*, *88*(C13), 8379–8400, doi:10.1029/JC088iC13p08379.

Cunnold, D. M., P. J. Fraser, R. F. Weiss, R. G. Prinn, P. G. Simmonds, B. R. Miller, F. N. Alyea, and A. J. Crawford (1994), Global trends and annual releases of CCl_3F and CCl_2F_2 estimated from ALE/GAGE and other measurements from July 1978 to June 1991, *J. Geophys. Res.*, *99*(D1), 1107–1126, doi:10.1029/93JD02715.

Derrick, M. R., H. D. Burgess, M. T. Baker, and N. E. Binnie (1990), Sulfuryl fluoride (Vikane): A review of its use as a fumigant, *J. Am. Inst. Conserv.*, *29*(1), 77–90, doi:10.2307/3179591.

Dillon, T. J., A. Horowitz, and J. N. Crowley (2008), The atmospheric chemistry of sulphuryl fluoride, SO_2F_2, *Atmos. Chem. Phys.*, *8*, 1547–1557.

Environmental Protection Agency (2004), Sulfuryl fluoride: Pesticide tolerance, *Fed. Regist.*, *69*(15), 3240–3257.

Environmental Protection Agency (2005), Sulfuryl fluoride: Pesticide tolerance, *Fed. Regist.*, *70*(135), 40,899–40,908.

Harnisch, J., M. Frische, R. Borchers, A. Eisenhauer, and A. Jordan (2000), Natural fluorinated organics in fluorite and rocks, *Geophys. Res. Lett.*, *27*(13), 1883–1886, doi:10.1029/2000GL008488.

Heise, H. M., R. Kurte, P. Fischer, D. Klockow, and P. R. Janissek (1997), Gas analysis by infrared spectroscopy as a tool for electrical fault diagnostics in SF_6 insulated equipment, *Fresenius J. Anal. Chem.*, *358*(7–8), 793–799, doi:10.1007/s002160050511.

Hobbs, J. P., and J. J. Hart (2005), Plasma cleaning gas with lower global warming potential than SF_6, report, Air Prod. and Chem., Inc., Allentown, Pa.

Holleman, A. F., and E. Wiberg (1985), *Lehrbuch der Anorganischen Chemie*, Walter de Gruyter, Berlin.

Hunt, G. R., and M. K. Wilson (1960), The infrared spectrum of sulfuryl fluoride, *Spectrochim. Acta Part A*, *16*(5), 570–574.

Jones, A. R., D. J. Thomson, M. Hort, and B. Devenish (2007), The UK Met Office's next-generation atmospheric dispersion model, NAME III, in *Air Pollution Modelling and Its Application*, vol. XVII, edited by C. Borrego and A.-L. Norman, pp. 580–589, Springer, New York.

Kettle, A. J., U. Kuhn, M. von Hobe, J. Kesselmeier, and M. O. Andreae (2002), Global budget of atmospheric carbonyl sulfide: Temporal and spatial variations of the dominant sources and sinks, *J. Geophys. Res.*, *107*(D22), 4658, doi:10.1029/2002JD002187.

Kóréh, O., T. Rikker, G. Molnár, B. M. Mahara, K. Torkos, and J. Borossay (1997), Study of decomposition of sulphur hexafluoride by gas chromatography/mass spectrometry, *Rapid Commun. Mass Spectrom.*, *11*(15), 1643–1648, doi:10.1002/(SICI)1097-0231(19971015)11:15<1643::AID-RCM14>3.0.CO;2-C.

Kranz, R. (1966), Organische Fluor-Verbindungen in den Gaseinschlussen der Wolsendorfer Flussspate, *Naturwissenschaften*, *53*(23), 593–600, doi:10.1007/BF00632268.

Krummel, P. B., R. Langenfelds, P. J. Fraser, L. P. Steele, and L. W. Porter (2007), Archiving of Cape Grim air, in *Baseline Atmospheric Program*

Australia 2005–2006, edited by J. M. Cainey et al., pp. 55–57, Aust. Bur. of Meteorol., Melbourne, Victoria, Australia.

Locarnini, R. A., A. V. Mishonov, J. I. Antonov, T. P. Boyer, and H. E. Garcia (2006), *World Ocean Atlas 2005*, edited by S. Levitus, 182 pp., *NOAA Atlas NESDIS*, vol. 61, NOAA, Silver Spring, Md.

Manning, A. J., D. B. Ryall, R. G. Derwent, and P. G. Simmonds (2003), Estimating European emissions of ozone-depleting and greenhouse gases using observations and a modeling back-attribution technique, *J. Geophys. Res.*, *108*(D14), 4405, doi:10.1029/2002JD002312.

Miller, B. R., R. F. Weiss, P. K. Salameh, T. Tanhua, B. R. Greally, J. Mühle, and P. Simmonds (2008), Medusa: A sample preconcentration and GC/MS detector system for in situ measurements of atmospheric trace halocarbons, hydrocarbons, and sulfur compounds, *Anal. Chem.*, *80*, 1536–1545, doi:10.1021/ac702084k.

Montzka, S. A., P. Calvert, B. D. Hall, J. W. Elkins, T. J. Conway, P. P. Tans, and C. Sweeney (2007), On the global distribution, seasonality, and budget of atmospheric carbonyl sulfide (COS) and some similarities to CO_2, *J. Geophys. Res.*, *112*, D09302, doi:10.1029/2006JD007665.

Morris, R. A., T. M. Miller, A. A. Viggiano, J. F. Paulson, S. Solomon, and G. Reid (1995), Effects of electron and ion reactions on atmospheric lifetimes of fully fluorinated compounds, *J. Geophys. Res.*, *100*(D1), 1287–1294, doi:10.1029/94JD02399.

Mühle, J., C. M. Harth, P. Salameh, B. R. Miller, R. F. Weiss, L. W. Porter, P. J. Fraser, and B. R. Greally (2006), Global measurements of atmospheric sulfuryl fluoride, *Eos Trans. AGU*, *87*(52), Fall Meet. Suppl., Abstract A53B–0191.

Orr, J. C., et al. (2005), Anthropogenic ocean acidification over the twenty-first century and its impact on calcifying organisms, *Nature*, *437*(7059), 681–686, doi:10.1038/nature04095.

Papadimitriou, V. C., R. W. Portmann, D. W. Fahey, J. Mühle, R. F. Weiss, and J. B. Burkholder (2008), Experimental and theoretical study of the atmospheric chemistry and global warming potential of SO_2F_2, *J. Phys. Chem. A*, *112*(49), 12,657–12,666, doi:10.1021/jp806368u.

Perkins, W. D., and M. K. Wilson (1952), The Infrared Spectrum of SO_2F_2, *J. Chem. Phys.*, *20*(11), 1791–1794, doi:10.1063/1.1700290.

Pest Management Regulatory Agency (2006), Sulfuryl fluoride, *Regul. Note REG2006–15*, Health Canada, Ottawa, Ont., Canada.

Pradayrol, C., A. M. Casanovas, I. Deharo, J. P. Guelfucci, and J. Casanovas (1996), Absorption coefficients of SF_6, SF_4, SOF_2 and SO_2F_2 in the vacuum ultraviolet, *J. Phys. III*, *6*(5), 603–612, doi:10.1051/jp3:1996143.

Pradayrol, C., A. M. Casanovas, C. Aventin, and J. Casanovas (1997), Production of SO_2F_2, SOF_4, (SOF_2 + SF_4), S_2F_{10}, S_2OF_{10} and $S_2O_2F_{10}$ in SF_6 and (50–50) SF_6-CF_4 mixtures exposed to negative coronas, *J. Phys. D Appl. Phys.*, *30*(9), 1356–1369, doi:10.1088/0022-3727/30/9/011.

Prinn, R. G. (2000), Measurement equation for trace chemicals in fluids and solution of its inverse, in *Inverse Methods in Global Biogeochemical Cycles*, *Geophys. Monogr. Ser.*, vol. 114, edited by P. Kasibhatla et al., pp. 3–18, AGU, Washington, D. C.

Prinn, R. G., et al. (2000), A history of chemically and radiatively important gases in air deduced from ALE/GAGE/AGAGE, *J. Geophys. Res.*, *105*(D14), 17,751–17,792, doi:10.1029/2000JD900141.

Prinn, R. G., et al. (2001), Evidence for substantial variations of atmospheric hydroxyl radicals in the past two decades, *Science*, *292*(5523), 1882–1888, doi:10.1126/science.1058673.

Prinn, R. G., et al. (2005), Evidence for variability of atmospheric hydroxyl radicals over the past quarter century, *Geophys. Res. Lett.*, *32*, L07809, doi:10.1029/2004GL022228.

Qu, J., H. Xu, and Z. Zhang (2000), Determination of sulfuryl fluoride in air by GC, *Fenxi Yiqi*, *2*, 32–34.

Ravishankara, A. R., S. Solomon, A. A. Turnipseed, and R. F. Warren (1993), Atmospheric lifetimes of long-lived halogenated species, *Science*, *259*(5092), 194–199, doi:10.1126/science.259.5092.194.

Seinfeld, J. H., and S. N. Pandis (1997), *Atmospheric Chemistry and Physics: From Air Pollution to Climate Change*, John Wiley, Hoboken, N. J.

Swedish Chemicals Agency (2005), Sulfuryl fluoride (PT8): Ecotoxicological profile including environmental fate and behaviour, *Competent Authority Rep. Doc. III-A7*, Sundbyberg, Sweden.

Symonds, R. B., W. I. Rose, and M. H. Reed (1988), Contribution of Cl^- and F-bearing gases to the atmosphere by volcanos, *Nature*, *334*(6181), 415–418, doi:10.1038/334415a0.

Takahashi, K., T. Nakayama, Y. Matsumi, S. Solomon, T. Gejo, E. Shigemasa, and T. J. Wallington (2002a), Atmospheric lifetime of SF_5CF_3, *Geophys. Res. Lett.*, *29*(15), 1712, doi:10.1029/2002GL015356.

Takahashi, T., et al. (2002b), Global sea-air CO_2 flux based on climatological surface ocean pCO_2, and seasonal biological and temperature effects, *Deep Sea Res., Part II*, *49*(9–10), 1601–1622, doi:10.1016/S0967-0645(02)00003-6.

United Nations Environment Programme (2004), Report of the Technology and Economic Assessment Panel (TEAP), progress report, May 2004, in *Montreal Protocol on Substances that Deplete the Ozone Layer*, p. 59, Nairobi.

United Nations Environment Programme (2006), *Handbook for the Montreal Protocol on Substances that Deplete the Ozone Layer*, Ozone Secr., Nairobi.

Wanninkhof, R. (1992), Relationship between wind speed and gas exchange over the Ocean, *J. Geophys. Res.*, *97*(C5), 7373–7382, doi:10.1029/92JC00188.

Weiss, R. F., and B. A. Price (1980), Nitrous oxide solubility in water and seawater, *Mar. Chem.*, *8*(4), 347–359, doi:10.1016/0304-4203(80)90024-9.

Whelpdale, D. M., and J. W. Miller (1989), GAW and precipitation chemistry measurement activities, *Fact Sheet 5*, Background Air Pollut. Monit. Program, World Meteorol. Org., Geneva.

Xiao, X., et al. (2007), Optimal estimation of the soil uptake rate of molecular hydrogen from the Advanced Global Atmospheric Gases Experiment and other measurements, *J. Geophys. Res.*, *112*, D07303, doi:10.1029/2006JD007241.

Yagi, K., J. Williams, N. Y. Wang, and R. J. Cicerone (1995), Atmospheric methyl-bromide (CH_3Br) from agricultural soil fumigations, *Science*, *267*(5206), 1979–1981, doi:10.1126/science.267.5206.1979.

Yates, S. R., D. Wang, J. Gan, F. F. Ernst, and W. A. Jury (1998), Minimizing methyl bromide emissions from soil fumigation, *Geophys. Res. Lett.*, *25*(10), 1633–1636, doi:10.1029/98GL51310.

P. J. Fraser, Centre for Australian Weather and Climate Research, CSIRO Marine and Atmospheric Research, Private Bag 1, Aspendale, VIC 3195, Australia. (Paul.Fraser@csiro.au)

B. R. Greally, S. O'Doherty, and P. G. Simmonds, School of Chemistry, University of Bristol, Cantock's Close, Clifton, Bristol, BS8 1TS, UK. (Brian.Greally@bristol.ac.uk; S.Odoherty@bristol.ac.uk; petergsimmonds@aol.com)

C. M. Harth, J. Mühle, P. Salameh, and R. F. Weiss, Scripps Institution of Oceanography, University of California, San Diego, 9500 Gilman Drive, La Jolla, CA 92093-0244, USA. (chris@gaslab.ucsd.edu; jens@gaslab.ucsd.edu; peter@gaslab.ucsd.edu; rfweiss@ucsd.edu)

J. Huang and R. G. Prinn, Department of Earth, Atmospheric and Planetary Sciences, Massachusetts Institute of Technology, Massachusetts Ave., Cambridge, MA 02139-4307, USA. (jhuang@mit.edu; rprinn@mit.edu)

B. R. Miller, Earth Systems, Research Laboratory, National Oceanic and Atmospheric Administration, Boulder, CO 80305-3337, USA.